

Diamond-like carbon for data and beer storage

Carbon is a very versatile element that can crystallize in the forms of diamond or graphite. There are many noncrystalline carbons, known as amorphous carbons. An amorphous carbon with a high fraction of diamond-like (sp^3) bonds is named diamond-like carbon (DLC). Unlike diamond, DLC can be deposited at room temperature. Furthermore, its properties can be tuned by changing the sp^3 content, the organization of the sp^2 sites, and the hydrogen content. This makes DLC ideal for a variety of different applications. We review the use of ultrathin DLC films for ultrahigh-density data storage in magnetic and optical disks and ultralong beer storage in plastic bottles.

Cinzia Casiraghi*, John Robertson, and Andrea C. Ferrari*

Cambridge University, Engineering Department, 9 JJ Thomson Avenue, Cambridge CB3 0FA, UK

*E-mail: cc324@cam.ac.uk; acf26@cam.ac.uk

Carbon-based materials play a major role in today's science and technology. Carbon is a very versatile element that can crystallize in the form of diamond and graphite. In recent years, there have been continuous and important advances in the science of carbon such as chemical vapor deposition of diamond¹ and the discovery of fullerenes², carbon nanotubes^{3,4}, and single-layer graphene⁵. There have also been major developments in the field of disordered carbons. In general, an amorphous carbon can have any mixture of sp^3 , sp^2 , and even sp^1 sites, with the possible presence of hydrogen and nitrogen. The compositions of nitrogen-free carbon films are conveniently shown on a ternary phase diagram (Fig. 1). An amorphous carbon with a high fraction of diamond-like (sp^3) bonds is known as diamond-like carbon (DLC). Unlike diamond, DLC can be deposited at room temperature, which is an important practical advantage. DLCs

possess an unique set of properties, which has lead to a large number of applications such as, for example, magnetic hard disk coatings; wear-protective and antireflective coatings for tribological tools, engine parts, razor blades, and sunglasses; biomedical coatings (such as hip implants or stents); and microelectromechanical systems⁶⁻¹⁰.

We first review the different varieties of DLCs. We then show how ultrathin DLC films enable ultrahigh-density data storage in magnetic and optical disks and ultralong shelf life for beer canned in plastic bottles. In the first case, up to ~ 1 Tbit/in² can be reached using sub-2 nm, atomically smooth films that act as a corrosion barrier to the recording medium. In the second case, hydrogenated amorphous carbons in the 100 nm thickness range provide a gas permeation barrier and enable standard polyethylene terephthalate (PET) bottles to efficiently store beer and carbonated soft drinks for tens of weeks.

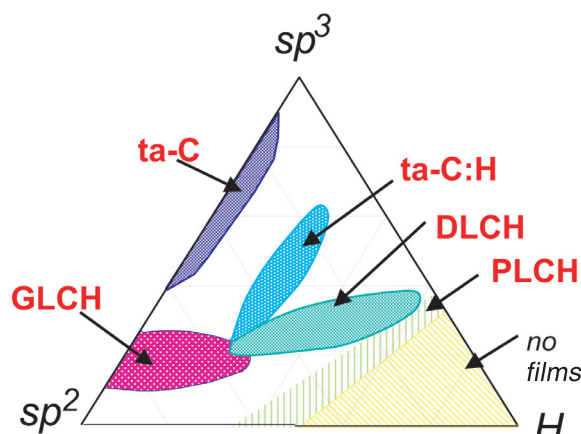


Fig. 1 Ternary phase diagram of amorphous carbons. The three corners correspond to diamond, graphite, and hydrocarbons, respectively. Depending on the sp^3 content and H content, DLC can be classified as: ta-C, which does not contain H and has a C-C sp^3 content greater than 60%; PLCH if the H content is greater than 40 at.% and sp^3 content is up to 70%; DLCH if H is 20-40 at.%; GLCH if H is below 20 at.% and the sp^3 content is lower than 20%. In ta-C:H, the sp^3 content can reach ~70% while the H content is 25-35% and the C-C sp^3 content is much greater than in PLCH. DLCH has a lower sp^3 content than ta-C:H, for a given H content.

The amorphous carbons family

One of the biggest hurdles in the amorphous carbon and DLC literature is understanding what exactly is referred to with these generic terms. Unfortunately, unlike carbon nanotubes, there are no simple indexes to easily classify these materials. Often films with completely different properties are called by the same name and vice versa. Thus, before working with them, we need to introduce by name each member of the amorphous carbon family. We also underline which carbon films can be produced by which deposition technique.

The key parameters are: (i) the sp^3 content; (ii) the clustering of the sp^2 phase; (iii) the orientation of the sp^2 phase; (iv) the cross-sectional nanostructure; and (v) the H or N content. Tetrahedral amorphous carbon (ta-C) is the DLC with the maximum C-C sp^3 content. This material can be grown with deposition techniques involving energetic ions, such as filtered cathodic vacuum arc (FCVA), mass-selected ion beam deposition (MSIBD), and pulsed laser deposition (PLD)¹⁰⁻¹⁶. The sp^3 content mainly controls the elastic constants¹⁷, but films with the same sp^3 and H content but different sp^2 clustering, sp^2 orientation, or cross-sectional nanostructure can have different optical and electronic properties¹⁸. As we move from ordered graphite to nanocrystalline graphite (nc-G) to amorphous carbon (a-C) and finally to sp^3 -bonded ta-C, the sp^2 groups become first smaller, then disordered, and finally change from ring to chain configurations¹⁸⁻²⁰. The evolution of the sp^2 phase clustering can be represented by the *amorphization trajectory*¹⁸⁻²⁰ (Fig. 2), consisting of three stages from graphite to ta-C. These are as follows: (i) graphite \rightarrow nc-G; (ii) nc-G \rightarrow sp^2 a-C; and (iii) a-C \rightarrow ta-C. Note how the sp^2 clustering evolution and sp^3 content evolution follow two distinct paths (Fig. 2b).

We classify hydrogenated a-C into four types, as shown in Fig. 1²¹:

1. a-C:H films with the highest H content (40-60 at.%). These films can have up to 70% sp^3 . However, most of the sp^3 bonds are H-terminated and the material is soft and has low density⁶. We call these films polymer-like a-C:H (PLCH). The bandgap ranges from 2-4 eV⁶. These films are usually deposited by plasma-enhanced chemical vapor deposition (PECVD) at low bias voltage²²⁻²⁴.
2. a-C:H films with intermediate H content (20-40 at.%). Even if these films have lower overall sp^3 content, they have more C-C sp^3 bonds than PLCH. Thus, they have better mechanical properties⁶. Their optical gap is between 1 eV and 2 eV⁶. We call these films

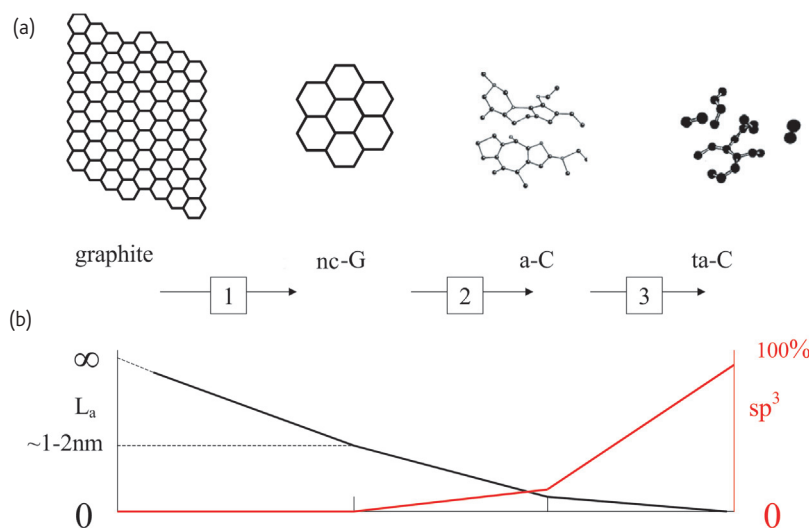


Fig. 2 (a) Variation of the sp^2 configuration along the three amorphization stages. (b) Schematic comparison of the evolution of the sp^2 cluster size (L_a ; black line) and sp^3 content (red line). Note that in stages (1) and (2), a strong sp^2 cluster size decrease corresponds to a relatively small sp^3 increase, while the opposite is seen in stage (3).

diamond-like a-C:H (DLCH). They are usually deposited by PECVD²¹⁻²³, electron cyclotron resonance (ECR), or reactive sputtering at moderate bias voltage^{21,23-27}.

3. Hydrogenated tetrahedral amorphous carbon films (ta-C:H) are a class of DLCH in which the C-C sp^3 content can be increased while keeping a fixed H content, as in Fig. 1. Many films defined in the literature as ta-C:H are just DLCHs. However, because of the higher sp^3 content (~70 %) and 25-30 at.% H, ta-C:H films are really a different category as indicated by their Raman spectra, higher density (up to 2.4 g/cm³), and Young's modulus (up to 300 GPa)^{17,28}. Their optical gap can reach 2.4 eV²⁹. These films are deposited by high-density plasma sources such as electron cyclotron wave resonance (ECWR)^{29,30}, and plasma beam source (PBS)^{31,32}.
4. a-C:H with low H content (less than 20 at.%). They have a high sp^2 content and sp^2 clustering. The gap is under 1 eV⁶. We call these films graphite-like a-C:H (GLCH). They are usually deposited by PECVD at high bias^{22,23} or magnetron sputtering²⁷.

Carbon nitrides are another important class of carbon films often used for tribological applications. As for hydrogenated amorphous carbons, it is possible to classify the bonding in carbon nitride films into four types, based on the bonding in the corresponding N-free films³³. The changes in the properties of the carbon nitride films as N content is increased should be compared with the properties of the corresponding N-free films. Thus, the variation of mechanical and electronic properties when N is added to an sp^2 -bonded carbon film differs from when N is added to a high sp^3 -content film. This is true whether H is present or not. There are four basic types of carbon nitride films, derived from sp^2 a-C, ta-C, a-C:H (from polymeric to diamond-like), and ta-C:H. Fig. 3 shows the ternary phase diagrams that summarize the compositions of carbon nitrides with increasing N content³³:

1. a-C:N. Here N is introduced into a-C films with a high fraction of sp^2 bonds. An unusual aspect of these films is that a-C:N deposited above 200°C can become nanostructured, with strong cross-linking between graphitic planes, which gives an increase in mechanical hardness and large elastic recovery³⁴⁻³⁷. This does not require, however, an increase of the sp^3 fraction (Fig. 3), but can rather be seen as an increase in disorder³⁵⁻³⁷. This effect is exploited in carbon nitrides used in magnetic storage, since the deposition of the carbon layer on the disk is performed at ~200°C, the process temperature resulting from the magnetic layer deposition.
2. ta-C:N. This group includes films deposited by MSIBD³⁸, PLD³⁹, or FCVA⁴⁰⁻⁴³ either under N₂ atmospheres or by N₂-assisted beams. Low-pressure deposition and high ionization ensure that film growth is controlled by ions. Resistivity and optical gap decrease when compared with pure ta-C films³³. Generally, the sp^3 content of ta-C remains high at 80-90% up to about 10% N, and then the sp^3 content and density fall rapidly³³. This sharp decrease is the result of the high deposition pressure⁴⁴. The sp^2 sites begin to cluster

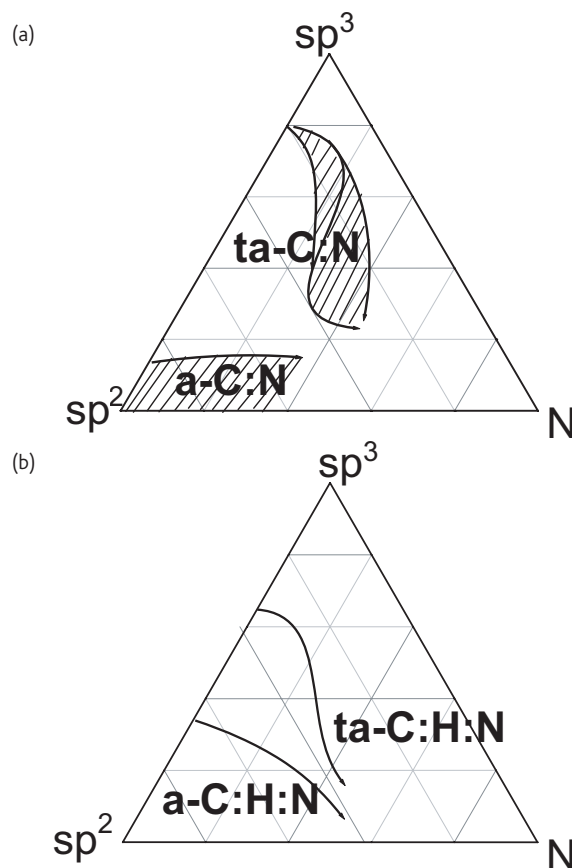


Fig. 3 Ternary phase diagrams of amorphous carbon nitride alloys: (a) without hydrogen; and (b) with hydrogen. ta-C:N (H) is obtained when N is introduced in a N-free film with a high sp^3 content, while a-C:N is obtained when N is introduced in graphitic N-free films. N has different effects depending on the sp^3 and sp^2 clustering of the N-free structure.

together at low N contents (1%) before the sp^3 to sp^2 transition, and this decreases the bandgap³³. Note that, although a general decrease of sp^3 content with N is observed, the trends are different according to the deposition systems³³. This implies that the evolution of the sp^3 fraction and the degree of clustering of the sp^2 phase can be different for films of the same N/C ratio³³.

3. a-C:H:N. These films are usually grown by PECVD⁴⁵⁻⁴⁷. a-C:H:N films have been deposited using a mixture of a hydrocarbon gas, such as methane, acetylene, benzene, and N₂ or NH₃. N incorporation is hindered if a high fraction of N₂ or a high substrate temperature is used. The best conditions for nitrogen incorporation correspond to the lowest H content in the gas phase. In contrast to a-C:N, the hardness in a-C:H:N films decreases with N, because of the formation of more terminating groups, such as NH₂ and nitrile³³. Higher substrate temperatures and substrate bias decrease the overall N and H content, giving a more graphite-like material. In principle, each a-C:H:N film can be further classified as DLCHN, PLCHN, or GLCHN by considering the properties of the 'host' a-C:Hs and their classifications, as described above.

4. ta-C:H:N. These films are prepared by a high-density plasma source, such as ECWR^{48,49}, ECR^{50,51}, or helicon sources⁵². Introducing N into ta-C:H induces clustering of the sp^2 phase, without an appreciable sp^3 to sp^2 conversion, up to ~20 at.% N, with a corresponding increase in conductivity and decrease of optical gap. Higher N contents cause a transition to a lower sp^3 fraction and give softer films similar to PLCHN³⁴.

There are then many other carbon films studied in literature, which evolve from the pattern presented so far. For example: (i) fluorinated DLCs are used as low dielectric constant insulators for improving the switching performances of circuits (see⁵³, for example). (ii) Amorphous carbon-silicon alloys ($a-C_{1-x}Si_x$) and hydrogenated carbon-silicon alloys ($a-C_{1-x}Si_xH_y$). These are studied both in the Si-rich and C-rich composition range⁵⁴. The Si-rich alloys have a wider bandgap than a-Si:H and are widely used as p -type window layers in a-Si:H based solar cells⁵⁵. The C-rich alloys are of interest as luminescent materials and as mechanical coating materials. The addition of Si to a-C:H has the beneficial effect of reducing the grown-in compressive stress, improving the thermal stability, and maintaining the low friction coefficient of a-C:H to a higher relative humidity^{54,56,57}. (iii) Metal-incorporated films to reduce stress and wear, as well as lowering friction (see⁵⁸, for example). (iv) Nanostructured sp^2 carbon films⁵⁹. These are attractive for electrochemical applications, supercapacitors, sensors, and fuel cells. They can be produced by cathodic arc or magnetron sputtering in the presence of a relatively high gas pressure to favor the aggregation of sp^2 clusters to be incorporated in the films. Supersonic cluster beam deposition can also be used to grow nanostructured thin films where the original carbon cluster structure is substantially maintained after deposition. Peculiar to these films is often the presence of carbon sp^1 chains⁵⁹.

Fig. 4a plots the relation between density and sp^3 content for ta-C, ta-C:H, and a-C:H films^{10,28}. In ta-C, many properties such as Young's modulus, hardness, density, and smoothness correlate directly with the C-C sp^3 fraction. An sp^3 increase is found to correspond linearly to a density increase according to¹⁰:

$$\rho \text{ (g/cm}^3\text{)} = 1.92 + 1.37F \quad (1)$$

where F is the sp^3 fraction between 0 and 1. It is also found that the Young's modulus E scales with the sp^3 fraction as¹⁰:

$$E \text{ (GPa)} = 478.5 (F + 0.4)^{1.5} \quad (2)$$

From eqs. 1 and 2, we can derive a general density versus Young's Modulus relation for ta-C:

$$\rho \text{ (g/cm}^3\text{)} = 1.37 + [E \text{ (GPa)}]^{2/3} / 44.65 \quad (3)$$

Fig. 4 plots experimental density and sp^3 fraction data and the general correlation resulting from eq. 3. Fig. 4b demonstrates that eq. 3 can be very efficiently used for ta-C.

DLC for magnetic storage

Hard disk drives are still the primary choice as archival mass data storage devices in computers and, in general, as high-performance

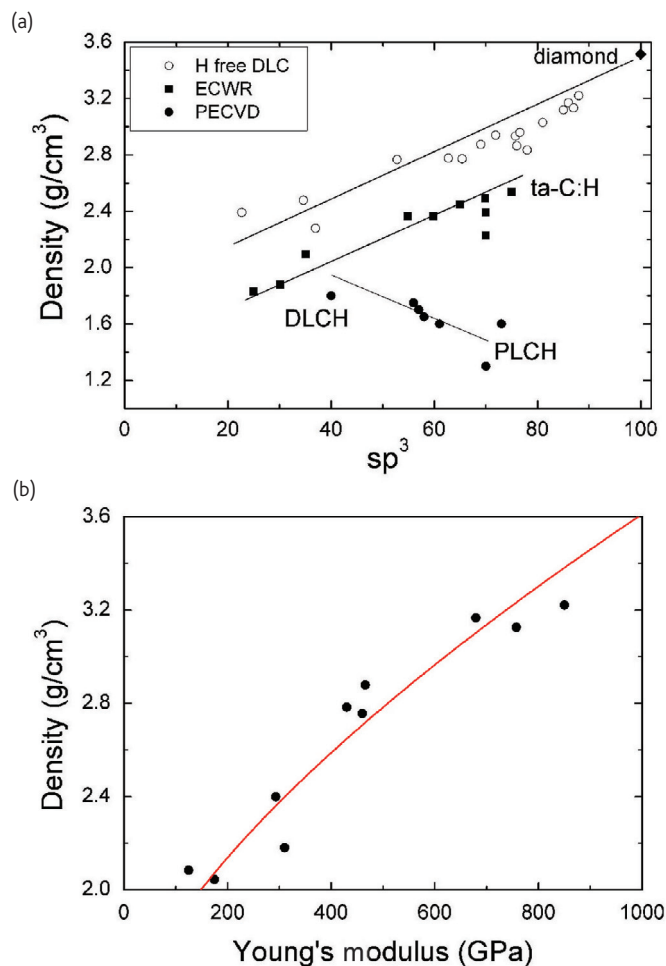


Fig. 4 (a) Density versus sp^3 fraction for N-free carbon films. Note the similar trends for ta-C and ta-C:H, but the opposite trend for a-C:H with increasing H content. (b) Density versus Young's modulus for ta-C films. The experimental trend can be well described by eq. 3, represented by the line in the plot.

storage devices. Magnetic storage technology has provided a constant increase in data storage density from 0.002 Mbits/in² in 1956 to 100 Gbits/in² in today's state-of-the-art drives⁶⁰.

In hard disks, the data are stored in a thin magnetic layer, called the recording medium, deposited on a substrate, usually Al or glass. A '1' bit is stored as a local magnetic moment in the direction of the recording data track, whereas a '0' bit corresponds to no change in the local moment orientation. This mode is referred to as longitudinal recording^{61,62}. The storage density is increased by reducing the area occupied by each bit of data. The areal density is the product of the tracks per inch and the bits per inch along a track⁶³. The ratio of tracks per inch and bits per inch is called the bit-aspect ratio. Initially, this ratio was approximately 20. The data storage density is limited by the bit size. Furthermore, the signal-to-noise ratio (SNR) depends on how many physical grains are included in one bit⁶⁴. Typically, SNR is linearly proportional to the number of grains per bit. Increasing areal density while preserving the SNR, therefore, requires reducing grain

size. However, the thermal activation of nanoscale magnetic particles, known as the superparamagnetic effect, precludes the continuous reduction in grain size because the thermal energy kT can overcome the coercive energy of the magnetic bit. This prevents further grain size reduction, or the SNR has to be compromised. In 1995, the storage density limit was approximately 40 Gbits/in². This was increased to 200 Gbits/in² by reducing the bit-aspect ratio to four and by using materials of higher coercivity^{60-63,65}. In principle, 1 Tbit/in² is possible, but using perpendicular recording, where the magnetization is normal to the film surface, in contrast to the standard longitudinal recording, where it is parallel to the surface^{60,61,64}. Indeed, recent demonstrations of perpendicular recording^{66,67} have reached 345-421 Gbit/in², with the potential for much higher values of 1 Tbit/in².

Another crucial bottleneck exists in order to reach the maximum storage density. Every hard disk has a DLC layer deposited over the magnetic layer to protect it against corrosion and wear^{10,63,68} (Fig. 5). The read/write head flies above the rotating disk on an aerodynamic bearing. It consists of many layers of thin films and is also protected by a DLC film (Fig. 5). An increase in the data storage density requires a magnetic recording configuration capable of writing very small magnetic grains and a signal processing system capable of recovering data reliably, since each bit is recorded on very few grains. This requires the significant reduction of the magnetic spacing, which is the vertical distance between the read head and the magnetic storage layer (Figs. 5 and 6). The magnetic spacing is slightly greater than the fly height, which is the separation of head and disk.

requires ever-thinner carbon films. These are presently ~4 nm thick. In order to achieve the goal of 1 Tbit/inch² in perpendicular recording, the magnetic spacing must be reduced to 6.5 nm, which implies a ~1 nm head and disk overcoat⁶⁹. This is only ~7 atomic layers thick, and the performance of such carbon films and the processes used to make them change dramatically when we approach these thicknesses.

The main challenge is thus the reduction of the coating thickness while maintaining its functional properties. The ideal carbon overcoat should be engineered to provide:

1. Corrosion protection, which requires complete coverage and high density;
2. Chemical properties, such as lube compatibility, stability, and low adsorption;
3. Surface topography, such as smoothness, complete coverage, and absence of particles;
4. Wear resistance, which requires reasonable hardness, low friction, and high elasticity; and
5. Magnetic layer integrity – the deposition process should minimize the 'dead layer' created by the impinging ion particles.

When first introduced, the role of carbon films was only to provide protection against corrosion, so simple a-C was used. Later, a-C:H was also used in order to provide protection against mechanical wear and damage during head crashes. More recently, a-C:N has been used instead of a-C:H. Nitrogen is usually found to have a beneficial effect on tribological properties⁷⁰. The deposition process generally used for disk coatings is magnetron sputtering. However, this is characterized by

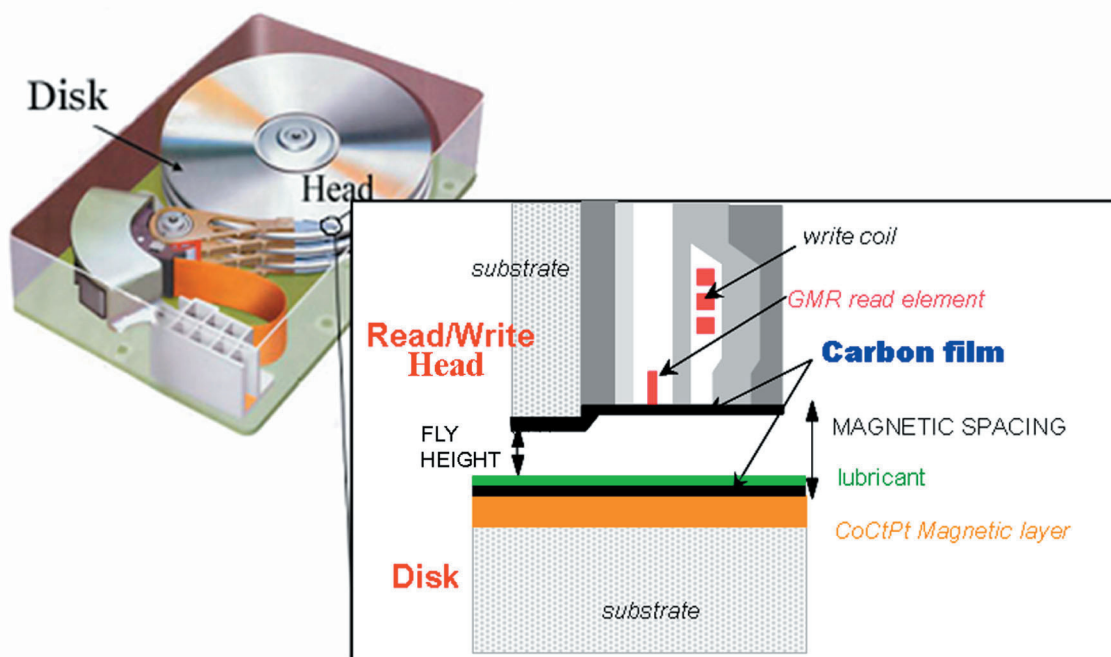


Fig. 5 Hard disk architecture.

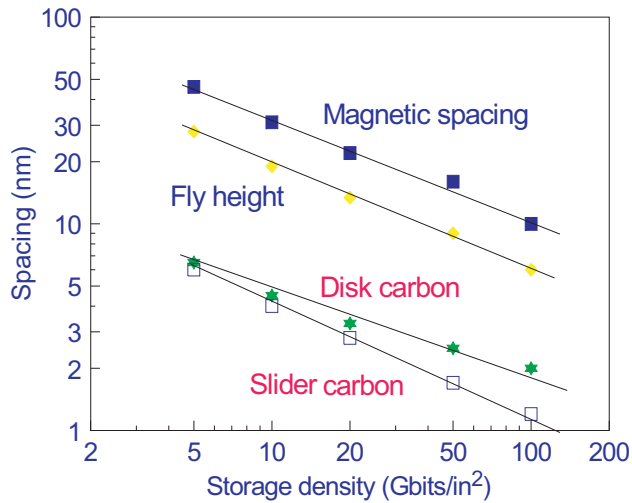


Fig. 6 Variation of carbon thickness on disk and sliders, magnetic spacing, and fly height with storage density (for longitudinal recording). For perpendicular recording, a given carbon thickness allows a much greater storage density, up to ~ 1 Tbit/in².

low energy and forms films of moderate density and hardness, failing to provide corrosion resistance for the ultrathin films required by next-generation hard disks⁷¹⁻⁷⁴. The ideal material for this would be ta-C because of its higher density and unique surface properties. The main drawback to the use of ta-C is the filtering of the macroparticles during deposition⁷⁵. These consist of graphitic clusters produced during arcing and, even in optimized conditions, can cover as much as 0.1% of the surface⁷⁵. If this problem is not satisfactorily solved, it may limit the use of ta-C to head production, where an acceptable yield of particle-free ta-C coated heads can already be achieved.

Analysis of ta-C roughness evolution has shown that ta-C has ultralow roughness (rms roughness ~ 0.12 nm) that is independent of the film thickness, thus providing films equally smooth whether 1 nm or 100 nm thick (Fig. 7)⁷⁶. These are unique properties since films usually form in a series of stages from nucleation, to coalescence, and possible roughening that, in general, lead to island formation for the thinnest films. The surface properties are correlated with the growth process, i.e. how the atoms arrive on the surface and how the layers grow. This can be studied by using the fractal theory of self-affine surfaces⁷⁷. A self-affine surface is scale-invariant under anisotropic transformations⁷⁷. Films deposited under nonequilibrium conditions are expected to have self-affine fractal surfaces since growth is the result of the competition between fluctuation and smoothing processes (excluding chemical reactions)⁷⁷. In film deposition, the fluctuations derive from the nonuniform nature of the incoming flux: the atoms reach the surface at random positions, with random time intervals between them. On the other hand, smoothing effects, such as thermal diffusion, tend to eliminate the height fluctuations. These two processes can only lead to a balancing effect on a relatively short-range scale and a kinetic roughening of the films occurs⁷⁷. This leads

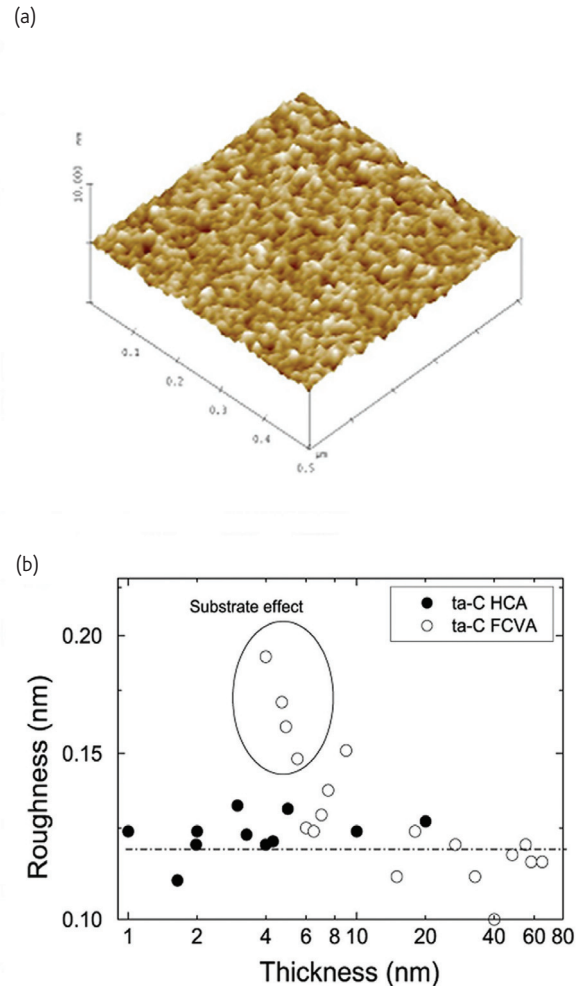


Fig. 7 (a) Atomic force microscope image of a 0.9 nm thick ta-C film. The scan size is 500 nm x 500 nm and the vertical scale is 10 nm. (b) Roughness as a function of the thickness for ta-C deposited with two different cathodic arc systems (high current arc, or HCA, and FCVA⁷⁶). In the case of ta-C deposited by FCVA, an exponential smoothing of the initial rougher substrate is observed.

the roughness R to scale with film thickness z as $R \sim z^\beta$. For a fixed thickness⁷⁷, R increases with the lateral length scale L as $R \sim L^\alpha$. The exponents α and β are called roughness and growth exponents and uniquely define a growth process⁷⁷. For ta-C, we found^{76,78} $\alpha = \beta = 0$. This corresponds to the Edwards-Wilkinson (EW) growth model⁷⁹. Here, the smoothing mechanism is diffusion driven by local surface curvature^{78,79}. Quantum and classical molecular simulations have shown that an efficient damping of surface fluctuations is achieved through impact-induced downhill currents, eroding hills on the film surface, in agreement with the EW model⁷⁸. This smoothing mechanism is able to explain several experimentally observed properties of ta-C growth⁷⁸. For example, it accounts for the smoothing of initially rough substrates. Starting from a sine-shaped film surface in Fig. 8a, the evolution of the surface was studied with classical

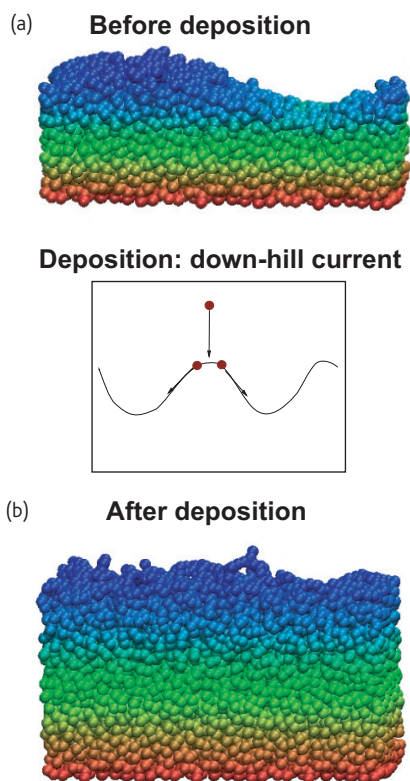


Fig. 8 Starting from a sine-shaped substrate surface (a), the evolution of the surface is studied with classical molecular dynamics during the impact of 4000 atoms. (b) Complete smoothing of the initial rough substrate after deposition⁷⁸. The color coding represents the height of the atoms.

molecular dynamics during the impact of 4000 atoms. Fig. 8b shows the complete smoothing of the initially rough film, in agreement with the experiments^{76,78}. This also explains why other carbon films, deposited at low ion energies, do not reach the ultra-smoothness of ta-C^{76,78}.

DLC for optical storage

Magnetic storage technology does not fully cover the required functionality of high-density portable storage devices. On the other hand, traditional optical storage systems such as CDs and DVDs cannot at present match the increasing storage capacity of hard disks. In an optical device, the digital information is encoded in surface structures, called pits and lands, with varying length⁸⁰⁻⁸² that modulate a readout light beam. Currently, the bits are obtained by focusing a laser beam with an objective lens on a transparent substrate or cover layer onto the highly reflective information layer. The data storage density depends on the number of bits per disk and, thus, on the bit size, which in turn depends on the laser spot size. The focused spot produced by the objective lens has a finite diameter and is limited to $\sim \lambda/2 \cdot \text{NA}$, where λ is the laser wavelength and NA is the numerical aperture of the lens (Fig. 9a). This is given by $n \cdot \sin \theta_{\text{max}}$, where n is the refractive index ($n = 1$ in air) and θ_{max} is the outer angle of the cone formed

by a converging beam of light. In a CD, NA is typically 0.4-0.5 and λ is 780 nm⁸⁰. In a DVD, NA is 0.6 and the recording λ is 650 nm⁸⁰. A third generation of optical devices has been made possible by the introduction of the blue diode laser in 1990, which allows a reduction of λ to 400 nm, and a storage density of 20-30 GB per disk⁸⁰. A fourth generation of optical devices aims to further increase the data storage density. There are several emerging technologies, such as holographic data storage, magneto-optical recording, and near-field data storage⁸⁰. In the latter cases, the solution requires a combination of the technologies used in optical and magnetic recording. In near-field technology, a dramatic reduction in the spot size can be achieved by using a lens with $\text{NA} > 1$, known as a solid immersion lens (SIL). The key concept is to replace air, which has a value of $n = 1$, with a material with $n > 1$, for example glass (Fig. 9b). It is possible to have a SIL with refractive index between 1.5 and 3⁸⁰. This will allow up to ~ 100 Gbytes per disk to be reached⁸². However, a gap of 20-30 nm between the lens and disk is needed⁸⁰. Thus, precise control over the size of the gap between lens and disk is required. This can be achieved with an air-bearing slider, similar to that commonly used in magnetic storage. The idea is to mount the lens on a slider, made of glass or plastic, which flies on a rotating disc.

The flying technology requires the use of a coating in order to protect slider and disk during start-stop and crashes. In the case of optical technology, the protective coating must:

1. Have good adhesion to glass or plastic sliders and the upper layer of the disk;
2. Be transparent at the laser recording wavelength (i.e. 400 nm);
3. Have low stress in order to avoid high waviness of the plastic substrate;
4. Be relatively dense and hard in order to provide protection against crashes;
5. Be resistant to the heat from the recording laser spot; and
6. Be compatible with the lubricant.

All these requirements can be satisfied by ta-C:H⁸³. Note that the need for transparency at 400 nm would require films with a bandgap of at least 3 eV, which is larger than the typical ta-C:H bandgap. However, since the target is to let the blue laser line go through the carbon coating, what really matters is the film transmittance rather than its

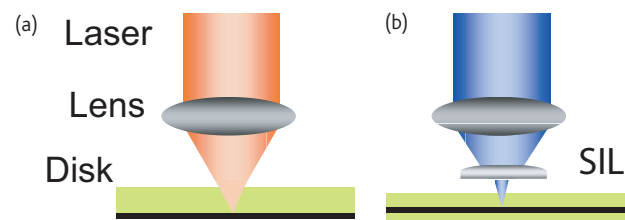


Fig. 9 (a) Current optical data storage technology, using far-field optics. (b) Near-field data storage technology using a SIL. CDs and DVDs use a metallic reflective layer (in black) sandwiched between a substrate (in green) and a lacquer surface (not shown).

optical gap. One way to increase the transmittance for a lower gap is to decrease the film thickness^{10,83}. Indeed, ta-C:H less than ~40 nm thick is transparent, relatively dense, hard, and can be deposited quickly and uniformly (70-80%) on the optical disk substrates⁸³.

DLC for beer storage

Poly(ethylene terephthalate) or PET is a very valuable plastic that can be blown into containers and bottles. PET has more flexibility in size and shape of packaging than metal cans. It is resealable, while metal cans are not, and easier to transport and handle than glass. Glass is breakable, heavy, and does not provide good portability. However, PET has a finite gas permeability that can limit the shelf life of some food and drink products. The addition of a gas-impermeable coating onto the inside wall of a standard PET bottle has long been considered as a way to improve the packaging for beer, fruit juice, and carbonated soft drinks, where the permeation of carbon dioxide, oxygen, and water needs to be suppressed (Fig. 10).

The International Society of Beverage Technologists defines the shelf life as the storage time corresponding to 17.5% loss of CO₂ for soft drinks and 10% loss of CO₂ for beer⁸⁴. The CO₂ loss during storage is not the only important factor in order to preserve the good taste of beer. Preventing beer from oxidation is also crucial⁸⁵. The maximum quantity of dissolved O₂ acceptable for beer is 1000 ppm, 50% from the head-space during the filling and the oxygen in the beer before the filling, and the other 50% permeating through the package⁸⁵.

The fruit juice and carbonated soft drinks markets are also concerned about the transparency of the coatings because most containers are transparent and the color of the coating may have some

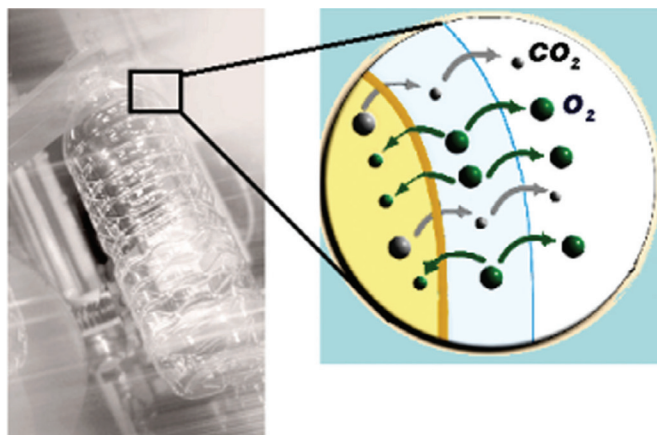


Fig. 10 PET has a finite gas permeability that can limit the shelf life of some food and drink products. The addition of a gas impermeable coating on the inside wall of a standard PET bottle is necessary in order to minimize the permeation of CO₂, O₂, and H₂O.

impact on processing conditions and the performance of bottles when using recycled PET material⁸⁶. A suitable coating must thus:

1. Have a relatively large atomic density;
2. Be deposited at a high rate to make a viable industrial process, but without exerting a large heat load, which would soften the PET substrate;
3. Be recyclable and food contact safe; and
4. Be optically transparent.

DLC, in principle, satisfies all these requirements. In addition, the optical bandgap can be varied over a wide range, so that it is possible to form an optically semitransparent coating on colored PET bottles, such as amber or green beer bottles, or a transparent coating for

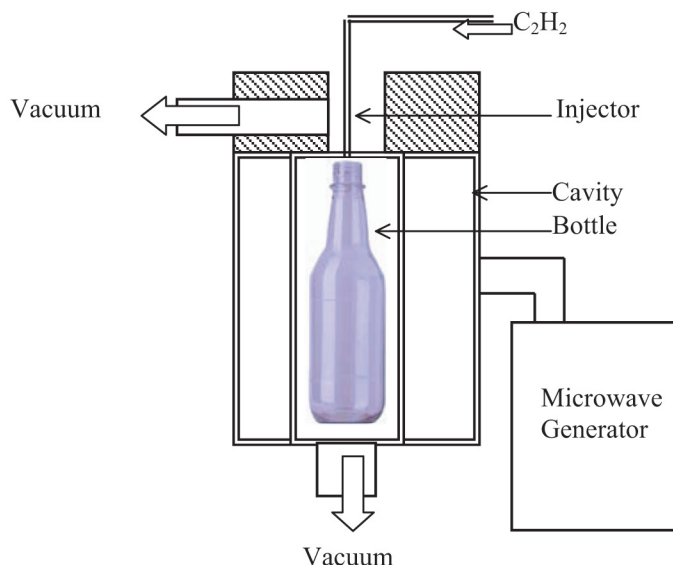


Fig. 11 Schematic of the system used to deposit DLC inside PET bottles⁸⁷. The bottle is first introduced into the treatment station, then vacuum is created inside and outside the bottle, acetylene gas is introduced into the bottle, and a plasma is generated by microwaves. Thus, DLC is deposited on the inner wall of the bottle. Finally, bottle and cavity are returned to atmospheric pressure and the bottle is extracted from the cavity.

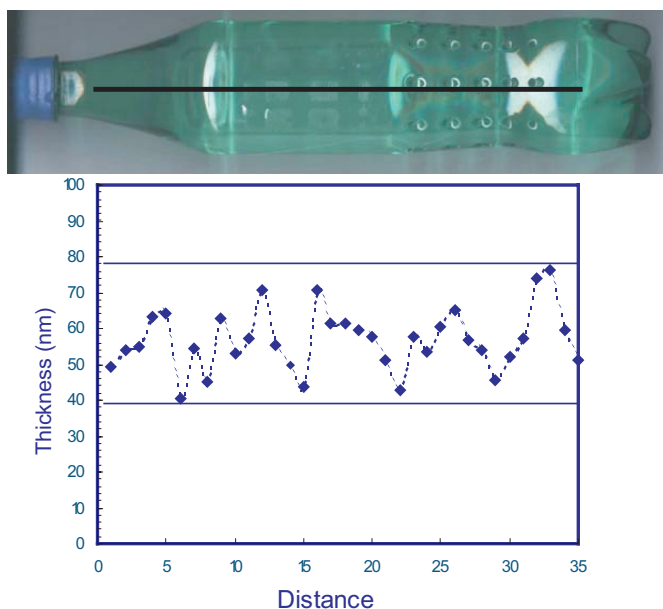


Fig. 12 The film thickness is found to be uniform within ~15% over the bottle interior. The thickness was measured on different areas of the PET bottle using a profilometer⁸⁷.

transparent bottles, such as those used for carbonated soft drinks or sparkling water. Ideally, ta-C would be the best material, but arc and PLD systems are not suited to coat the interior of plastic bottles. A plasma system, however, is ideal for this. Thus a-C:H is being used for this purpose⁸⁷⁻⁹⁰.

One solution currently on the market is to deposit a-C:H in PET bottles using a microwave plasma reactor⁸⁷, as shown schematically in Fig. 11. The bottle is placed neck-up inside the reactor. The pumping system creates a vacuum pressure of 50 mbar outside the bottle. At the same time, the inside of the bottle is pumped down to a pressure of around 0.1 mbar. This prevents the bottle from collapsing. An open-end tube is introduced inside the bottle to inject the acetylene process gas⁸⁷. A 2.45 GHz microwave discharge is ignited for 1-3 s at a power of 200-500 W to deposit the films⁸⁷. This allows a high deposition rate of 60 nm/s⁸⁷. This process has been industrially scaled to deposit 10 000 bottles/hour⁹¹. The films obtained with this process have a density of ~1.4 g/cm³, a thickness uniformity of 15%, and an optical gap of ~2.7 eV (Fig. 12)⁸⁷.

Fig. 13a shows that the oxygen transmission rate (OTR) through the bottle steeply decreases until a thickness of 40 nm and then levels off. The highest barrier for oxygen transmission is reached at ~150 nm. Further increase in the coating thickness does not reduce the OTR proportionally. The coating thickness is therefore chosen depending on the application. For a 100 nm a-C:H-coated bottle, the OTR is reduced to 0.0008 cc/package/24 hours from the 0.04 cc/package/24 hours of an uncoated PET bottle. Fig. 13b plots the CO₂ loss of a coated and an uncoated PET container as a function of storage time at 21°C. It

shows that for soft drinks an uncoated PET bottle has a ten week shelf life, while a coated one achieves a shelf life of 44-45 weeks. For beer, an uncoated bottle has a shelf life of just four weeks, while a coated one reaches 38 weeks⁸⁷. Currently, a shelf life exceeding 24 weeks can meet all distribution requirements. These performances can be further improved by increasing the thickness of the coating. Note that beer needs the highest oxygen transmission barrier. Thus, the thickest coating, 150 nm, is the optimum. Fruit juice and carbonated soft drinks need a medium gas barrier improvement with respect to uncoated PET. In this case, a thickness of 40-60 nm gives good performance.

The figures above are just an example of a solution recently developed and on the market^{87,91}. It is clear that moving toward ta-C:H will significantly reduce the thickness requirements.

Summary

The possibility to tune the structural, mechanical, and optical properties of a-C films makes them ideal for industrial implementation. Indeed, in the era of carbon nanotechnology, nanometer-thick DLC films are the only 'nanocarbon' components currently used in many every-day life applications. 

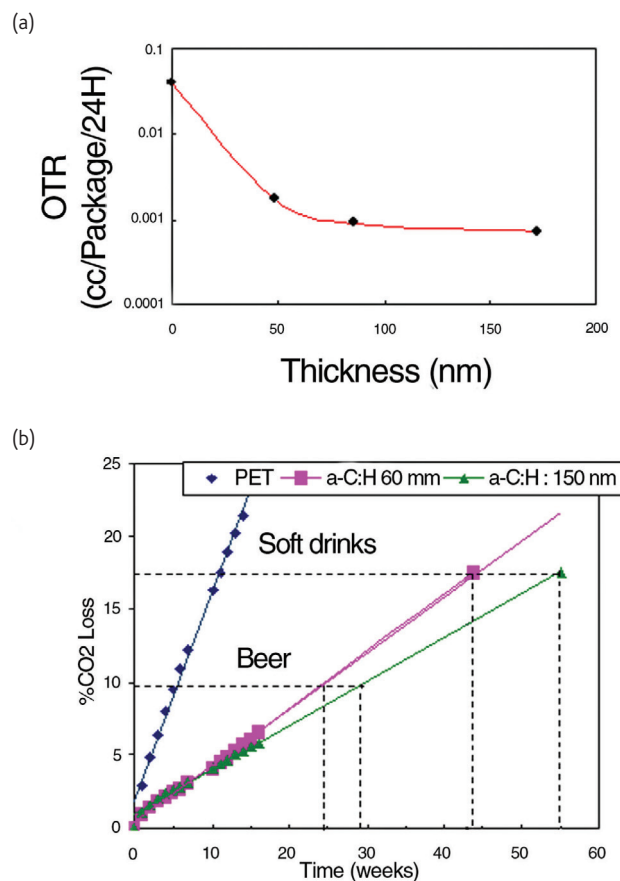


Fig. 13 (a) Oxygen transmission rate (OTR) versus film thickness. (b) CO₂ loss for 60 nm and 150 nm coated and noncoated PET bottles versus storage time.

Acknowledgments

The authors wish to thank the research team of the Mainz IBM STD plant: D. Schneider, R. Ohr, M. Von Gradowski, and H. Hilgers; M. Boutroy and the Sidel Group; C. Schug, D. Grambole, P. Gumbsch, and F. Piazza. We thank M. Moseler for the simulations in Fig. 8 and in the title page. Funding from

project 'Innovative Reaktoren und In-Situ Analytik für Nano-Schutzschichten' of the German Bundesministerium für Bildung und Forschung and the EU project 'Flyable media for slider based ultra high density optical recording' (FAMOUS) are acknowledged. CC acknowledges support from the Oppenheimer Fund. ACF acknowledges funding from the Royal Society and the Leverhulme Trust.

REFERENCES

- Angus, J. C., and Hayman, C. C., *Science* (1988) **241**, 913
- Kroto, H. W., et al., *Nature* (1985) **318**, 167
- Iijima, S., *Nature* (1991) **354**, 56
- Oberlin, A., et al., *J. Cryst. Growth* (1976) **32**, 335
- Novoselov, K. S., et al., *Science* (2004) **306**, 666
- Robertson, J., *Mater. Sci. Eng. R* (2002) **37**, 129
- Hauert, R., *Tribol. Int.* (2004) **37**, 991
- Sullivan, J. P., et al., *MRS Bull.* (2001) **26**, 309
- Luo, J. K., et al., *Appl. Phys. Lett.* (2004) **85**, 5748
- Ferrari, A. C., *Surf. Coat. Technol.* (2004) **180-181**, 190
- Lifshitz, Y., et al., *Phys. Rev. Lett.* (1994) **72**, 2753
- Voevodin, A., et al., *Surf. Coat. Technol.* (1997) **52**, 42
- Schwan, J., et al., *J. Appl. Phys.* (1996) **79**, 1416
- McKenzie, D. R., *Rep. Prog. Phys.* (1996) **59**, 1611
- Anders, S., et al., *Appl. Phys. Lett.* (1997) **71**, 3367
- Fallon, P. J., et al., *Phys. Rev. B* (1993) **48**, 4777
- Ferrari, A. C., et al., *Appl. Phys. Lett.* (1999) **75**, 1893
- Ferrari, A. C., and Robertson, J., *Phys. Rev. B* (2000) **61**, 14095
- Ferrari, A. C., and Robertson, J., *Philos. Trans. R. Soc. London, Ser. A* (2004) **362**, 2477
- Ferrari, A. C., and Robertson, J., *Phys. Rev. B* (2001) **64**, 075414
- Casiraghi, C., et al., *Phys. Rev. B* (2005) **72**, 085401
- Koidl, P., et al., *Mater. Sci. Forum* (1990) **52**, 41
- Tamor, M. A., et al., *Appl. Phys. Lett.* (1991) **58**, 592
- Yoon, S. F., et al., *J. Appl. Phys.* (2002) **91**, 1634
- Durand-Drouhin, O., et al., *J. Appl. Phys.* (2002) **91**, 867
- Schwarz-Sellinger, T., et al., *J. Appl. Phys.* (1999) **86**, 3988
- Popescu, B., et al., *J. Non-Cryst. Solids* (2000) **266-269**, 803
- Ferrari, A. C., et al., *Phys. Rev. B* (2000) **62**, 11089
- Morrison, N. A., et al., *Thin Solid Films* (1999) **337**, 71
- Weiler, M., et al., *Appl. Phys. Lett.* (1998) **1314**, 72
- Weiler, M., et al., *Phys. Rev. B* (1996) **53**, 1594
- Weiler, M., et al., *Appl. Phys. Lett.* (1994) **64**, 2797
- Ferrari, C., et al., *Phys. Rev. B* (2003) **67**, 155306
- Hellgren, N., et al., *Phys. Rev. B* (1999) **59**, 5162
- Jimenez, I., et al., *Phys. Rev. B* (2000) **62**, 4261
- Gammon, W. J., et al., *Phys. Rev. B* (2002) **66**, 153402
- Gammon, W. J., et al., *Phys. Rev. B* (2003) **68**, 195401
- Boyd, K. J., et al., *J. Vac. Sci. Technol. A* (1995) **13**, 2110
- Hu, J., et al., *Phys. Rev. B* (1998) **57**, 3185
- Davis, C. A., et al., *Phil. Mag. B* (1994) **69**, 1133
- Veerasingam, V. S., et al., *Phys. Rev. B* (1993) **48**, 17954
- Spaeth, C., et al., *Diamond Relat. Mater.* (1997) **6**, 626
- Kleinsorge, B., et al., *J. Appl. Phys.* (2000) **88**, 1149
- Rodil, S. E., et al., *Appl. Phys. Lett.* (2000) **77**, 1458
- Hammer, P., et al., *J. Vac. Sci. Technol. A* (1998) **16**, 2941
- Silva, S. R. P., et al., *J. Appl. Phys.* (1997) **81**, 2626
- Schwan, J., et al., *J. Appl. Phys.* (1998) **84**, 2071
- Rodil, S. E., et al., *J. Appl. Phys.* (2001) **89**, 5425
- Rodil, S. E., et al., *phys. status solidi a* (1999) **175**, 25
- Zhang, M., et al., *Jpn. J. Appl. Phys.* (1997) **36**, 4897
- Bhattacharyya, S., et al., *J. Appl. Phys.* (1998) **83**, 4491; Bhattacharyya, S., et al., *Diamond Relat. Mater.* (2000) **9**, 544
- Zhang, J. Q., et al., *Jpn. J. Appl. Phys.* (1997) **36**, 6894
- Grill, A., *Diamond Relat. Mater.* (2001) **10**, 234
- Racine, B., et al., *J. Appl. Phys.* (2001) **90**, 5002
- Matsuda, A., and Tanaka, K., *J. Non-Cryst. Solids* (1987) **97**, 1367
- Oguri, K., and Arai, T., *Thin Solid Films* (1992) **208**, 158
- Gangopadhyay, A. K., et al., *Tribol. Int.* (1997) **30**, 9
- Voevodin, A. A., et al., *Tribol. Int.* (1996) **29**, 559
- Milani, P., et al., *J. Appl. Phys.* (1997) **82**, 5793
- Coufal, H., et al., *MRS Bull.* (2006) **31** (5), 374
- Zhu, J.-G., *Materials Today* (2003) **6**, 22
- Menon, A. K., In *Proceeding Symposium on Interface Tribology Towards 100 Gbits/in²*, Bathia, C. S., et al., (eds.), The American Society of Mechanical Engineers, New York, (1999)
- Goglia, P. A., et al., *Diamond Relat. Mater.* (2001) **10**, 271
- Wood, R., *IEEE Trans. Magn.* (2000) **36**, 36; (2002) **38**, 1171
- Doerner, M. F., and White, R. L., *MRS Bull.* (1996) **9**, 28
- www.seagate.com
- www.hitachigst.com
- Robertson, J., *Thin Solid Films* (2001) **383**, 81; *Tribol. Int.* (2003) **36**, 405
- Gui, J., *IEEE Trans. Magn.* (2003) **39**, 716
- Yun, X., et al., *IEEE Trans. Magn.* (1997) **33**, 938
- Zhang, B., et al., *Data Storage* (1999) **1**, 25
- Tomcik, B., et al., *Diamond Relat. Mater.* (2002) **11**, 1409
- Bernhard, P., et al., *Surf. Coat. Technol.* (2004) **180-181**, 621
- Ohr, R., et al., *Surf. Coat. Technol.* (2003) **174-175**, 1135
- Teo, K. B. K., et al., *J. Appl. Phys.* (2001) **89**, 3707
- Casiraghi, C., et al., *Phys. Rev. Lett.* (2003) **91**, 226104
- Barabasi, A. L., and Stanley, H. E., *Fractal concepts in surface growth*, Cambridge University Press, Cambridge, UK, (1995)
- Moseler, M., et al., *Science* (2005) **309**, 1545
- Edwards, S., and Wilkinson, D., *Proc. R. Soc. London, Ser. A* (1966) **44**, 1039
- Coufal, H., and Dhar, L., *MRS Bull.* (2006) **31** (4), 294
- van Houten, H., and Schleipen, J., *Phys. World* (1998) **10**, 31
- Hellmig, J., *Phys. World* (2004) **17**, 21
- Piazza, F., et al., *Diamond Relat. Mater.* (2005) **14**, 994
- International Society of Beverage Technologists, *Voluntary Test Methods for PET bottles*, Revision 1, (2003)
- Huige, N. J., *ACS Symp. Ser.* (1993) **563**, 64
- National Association for PET Container Resources, *Annual report on post consumer PET container recycling activity*, (2004)
- Boutroy, N., et al., *Diamond Relat. Mater.* (2006) **15**, 921
- Abbas, G. A., et al., *Carbon* (2005) **43**, 303
- Yoshida, M., et al., *Surf. Coat. Technol.* (2003) **174-175**, 1033
- Yamamoto, S., et al., *Diamond Relat. Mater.* (2005) **14**, 1112
- www.sidel.com